 DOI: 110.31276/VJSTE.2023.0012

# Optimisation of calcinothermic reduction for metallic dysprosium preparation

**Nguyen Trong Hung*, Nguyen Thanh Thuy, Le Ba Thuan**

*Institute for Technology of Radioactive and Rare Elements, 48 Lang Ha Street, Lang Ha Ward, Dong Da District, Hanoi, Vietnam*

Received 21 February 2023; revised 23 May 2023; accepted 15 February 2024

***Abstract:***

**This research focuses on optimising the process of preparing metallic dysprosium through calcinothermic reduction. The study employed response surface methodology (RSM) based on a central composite face-centred (CCF) design to model the interactive effects of three independent variables: reduction temperature, Ca/$DyF_3$ molar ratio, and reduction time, on the dependent response, which was the reduction yield. Initially, experiments were conducted to determine the experimental matrix or planning region. Subsequently, experimental studies were carried out within this matrix to develop a quadratic response surface methodology - central composite face (RSM-CCF) model for the calcinothermic reduction of $DyF_3$ using MODDE 5.0 software. The resulting model demonstrated good agreement between calculated and actual data, establishing a reliable framework for the calcinothermic reduction process. Further analysis involved assessing the contributions of the model's coefficients to the dependent response to optimise the process. The findings indicate that reduction temperature plays a significant role in governing the calcinothermic reduction. The optimal parameters for the calcinothermic reduction of $DyF_3$ were identified as a reduction temperature of 1450-1460°C, a reduction time of 50 minutes, and a Ca/$DyF_3$ molar ratio of 2.15. Under these conditions, the maximum reduction yield achieved was 85.7%.**

***Keywords:*** **calcinothermic reduction, metallic dysprosium, modelling, optimising.**

***Classification numbers:*** **2.2, 2.3, 4.2**

## 1. Introduction

Dysprosium (Dy) is a valuable heavy rare earth element. Along with iron and terbium, Dy is a component of the magnetic material Terfenol-D ($Tb_xDy_{1-x}Fe_2$; $x \approx 0.3$), which exhibits the highest room-temperature magnetostriction of any known material. Dy is also a critical component in the production of high-energy permanent magnets, such as Nd-Fe-B ($Nd_{13.4-x}Dy_{0.2+x}Fe_{79.7}M_{0.4}B_6$; x = 0-0.3; M is Co or Cu), which are used in modern electrical generators and motors for hybrid and electric vehicles, as well as wind turbine generators. Nearly 95% of the total demand for Dy is for its use in Nd-Fe-B permanent magnets. Additionally, Dy is required in hard disc drives, transducers, wide-band mechanical resonators, and high-precision liquid-fuel injectors. In the nuclear sector, Dy has a high thermal-neutron absorption cross-section, and consequently, dysprosium-oxide-nickel CERMET material is used as neutron-absorbing control rods in nuclear reactors. Dy is also utilised in dosimeters for measuring ionising radiation [1-3].

In metallurgy, molten salt electrolysis and metallothermic reduction are the two main techniques for producing rare earth metals. Light rare earth metals, such as lanthanum (La), cerium (Ce), praseodymium (Pr), and neodymium (Nd), which have low melting points (920, 795, 935, and 1024°C, respectively), are commonly produced via molten salt electrolysis. In contrast, heavy rare earth metals such as Dy and Tb, with higher melting points (1407 and 1356°C, respectively), are typically produced using metallothermic reduction [4-7].

Both techniques employ anhydrous free-oxygen chloride or fluoride rare earth salts as feed materials. Although the salt electrolysis or metallothermic reduction temperature of anhydrous free-oxygen chloride salts is lower than that of fluoride salts, chloride salts have a highly hygroscopic nature, which is a major disadvantage. In contrast, anhydrous free-oxygen fluoride rare earth salts are preferred due to their superior stability. The metallothermic reduction of anhydrous free-oxygen fluoride salts using metallic calcium as the reductant is known as calcinothermic reduction [8].

The production of metallic rare earth by molten salt electrolysis or metallothermic reduction involves two key steps: (i) fabrication of anhydrous free-oxygen fluoride and (ii) molten salt electrolysis or calcinothermic reduction of the anhydrous fluoride to obtain metallic rare earth. In the case of Dy, metallic dysprosium is fabricated by the calcinothermic reduction of anhydrous free-oxygen fluoride Dy, which can be produced from, for example, the

*Corresponding author: Email: nthungvaec@gmail.com

fluorination of dysprosium oxide ($Dy_2O_2$) using ammonium bifluoride ($NH_4HF_2$) [9-11]. Previous studies have reported the fluorination of dysprosium oxide, terbium oxide ($Tb_4O_7$), and terbium chloride ($TbCl_3$) using ammonium bifluoride for the preparation of anhydrous free-oxygen fluoride dysprosium and terbium [12-14]. However, to the authors' knowledge, no previous study has investigated the calcinothermic reduction of $DyF_3$ for the preparation of metallic Dy.

This study aims to fill this research gap by investigating and optimising the calcinothermic reduction process of anhydrous free-oxygen $DyF_3$ to obtain metallic Dy. The relevant process parameters influencing the yield of calcinothermic reduction were identified using an Ishikawa diagram, which depicted various factors affecting the reduction yield of $DyF_3$, including material factors (e.g., purity of $DyF_3$, metallic Ca, powder form), equipment factors (e.g., tooling conditions, scale accuracy, temperature profile, calibration), and process parameters (e.g., reduction temperature, reduction time, Ca/$DyF_3$ molar ratio, moisture, inert gas environment).

The primary process parameters identified for investigation were reduction temperature, reduction time, and Ca/$DyF_3$ molar ratio. Subsequently, the quantitative relationship between these parameters and the reduction yield was evaluated. The RSM approach, based on CCF design, was employed to empirically model the interactions between the process parameters (independent variables) and the calcinothermic reduction yield (dependent response). This approach facilitated the optimisation of the process by identifying the optimal values for each variable and reducing the number of experiments required. Ultimately, the regression model developed through RSM enabled accurate prediction of the reduction process outcomes and optimisation accordingly.

## 2. Materials and methods

### *2.1. Preparation of dysprosium fluoride ($DyF_3$) material*

Dysprosium oxide ($Dy_2O_3$) with a purity of 99.9% was obtained from dysprosium chloride ($DyCl_3$) solution, which resulted from the separation and purification of total rare earth oxides (TREO) from Yen Phu, Vietnam, using the solvent extraction method. The extraction was carried out using PC88A as the extractant at the Institute for Technology of Radioactive and Rare Elements (ITRRE) [15-18]. The procedure for $Dy_2O_3$ preparation is as follows: the $DyCl_3$ solution was first precipitated using a saturated oxalic acid solution; chloride ($Cl^-$) anions were then completely removed from the dysprosium oxalate [$Dy_2(C_2O_4)_3$] precipitate using dilute oxalic acid as a scrubbing solution. The resulting dysprosium oxalate was then annealed in air at 600°C for 2 hours, converting the oxalate salts into dysprosium oxide. The fluorinating reagent used was ammonium bifluoride ($NH_4HF_2$), with a purity of ≥99% (purchased from Shanghai Epoch Material Co., Ltd).

A mixture of $NH_4HF_2$ and $Dy_2O_2$ in a stoichiometric ratio of 3.5:1 was prepared using laboratory ceramic ball mill grinding equipment for approximately 0.5 hours. The fluorination of $Dy_2O_3$ by $NH_4HF_2$ is a solid-phase chemical reaction, requiring sufficient contact between the reactants to optimise performance. To achieve this, the mixture of $Dy_2O_3$ and $NH_4HF_2$ was ground into smaller particles, increasing the surface area and enhancing contact between the solid phases. This process improved the fluorination yield, leading to higher conversion rates and more efficient reactions. The reduction of particle size also promoted a uniform distribution of reactants, minimising local concentration gradients and enabling more homogeneous reactions. Therefore, reducing particle size plays a crucial role in solid-phase chemical reactions, significantly impacting their efficiency and effectiveness.

The fluorination was carried out in a tube furnace (Nabertherm) at 350-450°C for 3 hours. Upon loading the mixture into the furnace, it was necessary to vent the steam produced during the reaction to maintain stable furnace conditions. A water aspirator was attached to the outlet of the furnace, while two compressed air cylinders with pressure-reducing valves were connected to the furnace inlet. These measures ensured a continuous flow of compressed air, removing the steam produced during the reaction and maintaining appropriate temperature and pressure conditions. This approach facilitated a smooth reaction process and the production of high-quality fluorinated products. The flow of compressed air also enhanced safety and efficiency, minimising the risk of overheating or other hazards that could compromise the process. As a result, the conversion efficiency of the oxide to fluoride was estimated to be over 99%.

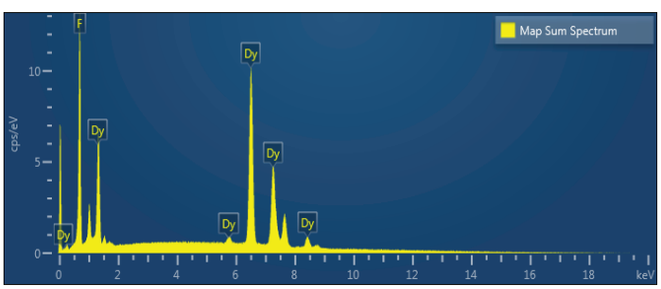


**Fig. 1. The EDS pattern of $DyF_3$** [12].

Analysis of the data presented in Fig. 1 reveals no detectable peaks corresponding to oxygen in the EDS pattern. Furthermore, the calculated compositions of the F and Dy elements, based on the [$DyF_3$] formula, closely match those determined from the EDS results. These findings confirm the successful conversion of $Dy_2O_2$ into

the desired [$DyF_3$] product. The absence of oxygen peaks further indicates that the reaction proceeded to completion, leaving no residual oxygen in the final product. Overall, the results provide strong evidence that the fluorination process effectively produced high-quality [$DyF_3$] with accurate and consistent elemental compositions in line with the intended formula. The anhydrous $DyF_3$ is used as the raw material for the calcinothermic reduction to produce metallic dysprosium (Dy).

### *2.2. Chemicals and equipment*

Metallic calcium clinkers (99% pure, 1 mm in size), stored under inert gas, were used as a reductant (purchased from Shanghai Epoch Material Co., Ltd). A 15 kW induction furnace, with a maximum operating temperature of 1800°C (Zhengzhou, China), was utilised for the reduction process (Fig. 2). The furnace consisted of a sealed silica chamber, approximately 180 mm in length, housing a graphite susceptor with a diameter of 80 mm. The susceptor featured a central hole in its lid. The reaction occurred inside a tantalum crucible placed within the susceptor for indirect heating.

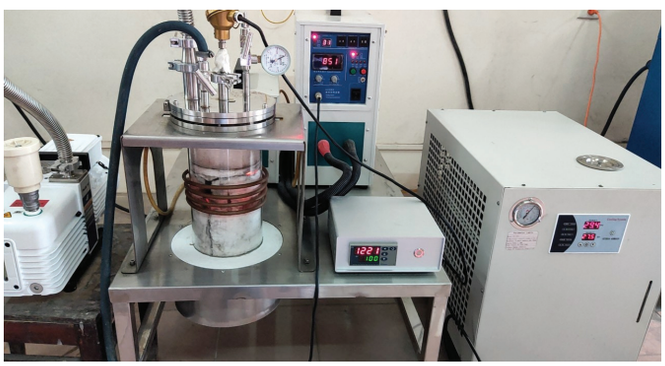

**Fig. 2. The vacuum inductive furnace.**

Temperature measurements were conducted using a two-colour pyrometer, directed at the central hole of the graphite susceptor lid. While no black body correction was applied, the ratio of the distance between the susceptor lid and the charged surface to the diameter of the hole was approximately 4-5. Although this configuration did not create a perfect black body, the recorded temperatures were reasonably close to the actual values, ensuring practical significance. The furnace employed a proportional-integral-derivative (PID) control mechanism, receiving temperature data from the pyrometer. This setup enabled precise and controlled heating with an accuracy of ±2°C, even in an induction furnace. Additionally, the pyrometer allowed observation of changes in the charge throughout the process, despite the sealed system.

Prior to heating, the furnace chamber was purged with argon at a flow rate of approximately 2 l/min for a sufficient period. This slight flow of argon, maintained via a bubbler, continued throughout the entire reduction process.

### *2.3. Experiments*

(i) Sample preparation: 50 g of dry $DyF_3$ and a specified weight of metallic calcium were placed in a tantalum crucible with a volume of 100 ml. The mixture was stirred for 2 hours in a laboratory box filled with argon gas, after which the crucible was placed in the vacuum induction furnace.

(ii) Calcinothermic reduction of $DyF_3$: The process was conducted at temperatures ranging from 1200 to 1500°C, with a $Ca/DyF_3$ molar ratio of 1.65-2.25, for 0.25-1 hour. Upon completion, metallic Dy in the reduction samples was dissolved in diluted hydrochloric acid (HCl), and Dy content in the solution was determined using an inductively coupled plasma optical emission spectrometer (ICP-OES, Horiba, Japan). The reduction yield was calculated based on the Dy content in the original $DyF_3$ and in the solid after reduction, as follows (Eq. 1):

$$\text{Reduction yield (\%)} = \frac{\text{Initial Dy} - \text{Dy in solid}}{\text{Initial Dy}} \times 100 \quad (1)$$

A satisfactory mass balance was achieved for each reduction experiment, with five replications performed for each experiment.

### *2.4. Modeling*

The method of modelling and statistical design of experiments, using a central composite face-centred (CCF) design in response surface methodology (RSM), was employed [15]. The dependent response in this study was the reduction yield (Y, %), while the independent variables, or factors, were the reduction temperature ($X_2$, °C), $Ca/DyF_3$ molar ratio ($X_2$, mol/mol), and reduction time ($X_2$, h). The levels of these variables are presented in both coded and actual values in Table 1.

**Table 1. Independent variables and their corresponding levels.**

| Independent variable | Symbol coded | Coded variable levels | | |
|---|---|---|---|---|
| | | *-1* | *0* | *1* |
| Reduction temperature (°C) | $X_1$ | 1400 | 1450 | 1500 |
| $Ca/DyF_3$ molar ratio (mol/mol) | $X_2$ | 1.95 | 2.10 | 2.25 |
| Reduction time (h) | $X_3$ | 0.50 | 0.75 | 1.00 |

To determine the optimal combination of these factors for achieving the highest reduction yield, 15 experimental runs were required. This was calculated as $2k+2k+n_0$, where k is the number of factors, in this case three, and $n_0$ is the number of replications at the centre points, set to one for this study. Therefore, 15 runs were necessary to obtain sufficient data for analysis and to identify the most effective combination of reduction temperature, $Ca/DyF_3$ molar ratio,

and reduction time for maximising the reduction yield. By carefully controlling these variables, it is possible to optimise the reduction process and maximise the production of high-quality reduced products.

The experimental results were entered into MODDE 5.0 software, which was used to fit the model via multiple linear regression. This process employed an RSM-CCF regression model, mathematically represented as follows Eq. 2:

$$Y = b_0 + \sum_{i=1}^{k} b_i X_i + \sum_{i=1}^{k} b_{ii} X_i^2 + \sum_{i,j=1(i\neq j)}^{k} b_{ij} X_i X_j \qquad (2)$$

where Y is the dependent response; $b_0$ is the constant coefficient; $b_i$, $b_{ii}$ and $b_{ij}$ are the linear, quadratic, and interaction coefficients, respectively; $X_i$ and $X_j$ are the coded values of the independent variables; $X_iX_j$ and $X_i^2$ represent the interaction and quadratic terms, respectively.

By applying this model to the experimental data, a deeper understanding of the relationships between the independent variables (factors) and the dependent response (reduction yield) was obtained. This information can be used to optimise the reduction process and improve the quality of the reduced products. The use of advanced statistical modelling techniques, such as multiple linear regression and RSM-CCF, is essential for achieving accurate and reliable results in experimental research, significantly enhancing the understanding of complex processes and systems.

## 3. Results and discussion

### *3.1. Determining the experimental planning region*

A central composite face-centred (CCF) design, within the framework of response surface methodology (RSM), is capable of modelling the linear, quadratic, and interaction effects of independent variables on the dependent response. Thus, incorporating a model based on the CCF design provides a comprehensive understanding of the overall reduction process, leading to an accurate description of the system under investigation. Prior to implementing the CCF design in RSM for modelling the calciothermic reduction process, experimental studies were conducted to examine the effects of the independent variables on the dependent response. These studies are essential in determining the experimental planning region, which is necessary for obtaining accurate and reliable results.

By conducting these experimental studies and defining the planning region, a CCF design can be effectively used to model the calciothermic reduction process. This facilitates the optimisation of process parameters, thereby improving the quality of the final product and enhancing efficiency and productivity. The calciothermic reduction reaction of $DyF_3$ is shown in equation (3):

$$\frac{3}{2}Ca + DyF_3 = Dy + \frac{3}{2}CaF_2 \qquad (3)$$

From the literature, the key parameters influencing the calciothermic reduction are reduction temperature, Ca/$DyF_3$ molar ratio, and reaction time. Studies investigating the effects of these parameters on the reduction yield were undertaken.

The investigation into the effect of reduction temperature on the reduction yield was conducted at a Ca/$DyF_3$ molar ratio of 2.1 and a reduction time of 0.5 hours. The results indicated that at temperatures below 1300°C, the reduction yield was very low (<10%). At 1300°C, the yield increased to 35%, while in the temperature range of 1400 to 1500°C, the reduction yield reached approximately 80%.

The study on the effect of Ca/$DyF_3$ molar ratio on the reduction yield was conducted at a fixed reduction temperature of 1450°C and a reduction time of 0.5 hours. The reduction yields at Ca/$DyF_3$ molar ratios of 1.65, 1.84, 1.95, 2.1, and 2.25 were 54.3±0.8, 62.1±1.0, 80.8±1.2, 84.6±1.0, and 85.4±0.6%, respectively.

The investigation into the effect of reduction time on the reduction yield was carried out at a fixed Ca/$DyF_3$ molar ratio of 1.95 and a reduction temperature of 1400°C. The reduction yields for time intervals of 0.25, 0.5, 0.75, and 1 hour were 71.9±1.4, 73.3±1.6, 75.4±1.0, and 75.2±1.2%, respectively.

The effects of reduction temperature, Ca/$DyF_3$ molar ratio, and reduction time on the reduction yield of $DyF_3$ by metallic calcium are illustrated in Fig. 3. Based on these results, the planned experimental region was determined as follows: reduction temperatures of 1400-1500°C, Ca/$DyF_3$ molar ratios of 1.95-2.25, and reduction times of 0.5-1 hour. The subsequent experimental studies to model the calciothermic reduction of $DyF_3$ were implemented within this defined region.

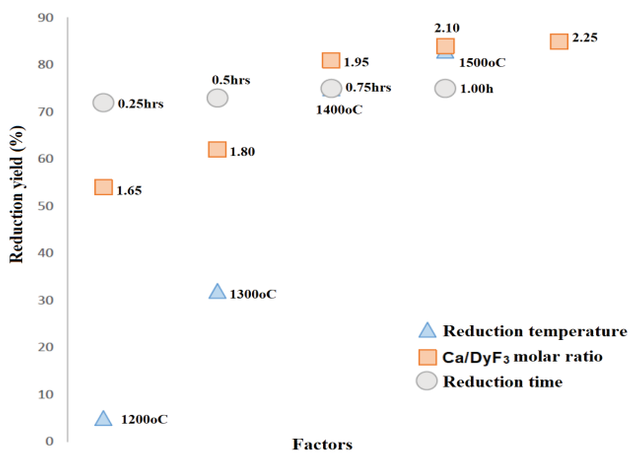


**Fig. 3. The effects of factors on the reduction yield of $DyF_3$ by metallic calcium.**

### *3.2. Modelling the calcinothermic reduction of $DyF_3$*

A response surface methodology (RSM) with a CCF design was employed to evaluate the impact of independent variables on the dependent response, specifically the reduction yield. The study examined the effects of three variables: reduction temperature (ranging from 1400 to 1500°C), $Ca/DyF_3$ molar ratio (ranging from 1.95 to 2.25), and reduction time (ranging from 0.5 to 1 hour).

To accurately represent the relationship between these variables and the reduction yield, a quadratic model was selected, denoted by the variable Y. The MODDE 5.0 software was used to guide the adoption of this robust model, facilitating the analysis of the experimental data. Through this approach, optimal values for each independent variable were determined, enabling maximisation of the reduction yield and improving process efficiency.

In the RSM-CCF model, the independent variables were assigned codes for ease of analysis. Reduction temperature, $Ca/DyF_3$ molar ratio, and reduction time were designated as $X_1$, $X_2$, and $X_3$, respectively. A coding scheme was applied, where high, centre, and low levels were represented by 1, 0, and -1, respectively, as shown in Table 2. This coding approach was crucial for conducting accurate experimental studies and modelling the effects of independent variables on the dependent response. By employing codes and levels, a structured and systematic framework was established, enhancing the accuracy and reliability of the results obtained.

The outcomes of the 15 experimental runs were recorded in Table 2 and input into the MODDE 5.0 software for further analysis. Using multiple linear regression, the software fitted a model to the experimental data, providing a comprehensive understanding of the factors influencing the dependent response. Furthermore, this model can be utilised for predicting the outcomes of future experiments and optimising the reduction process.

To evaluate the adequacy of the quadratic model in the calciothermic reduction of $DyF_3$, a significance test and analysis of variance (ANOVA) were conducted. Table 3 provides a summary of the estimated regression coefficients, along with their corresponding 95% confidence intervals. The accuracy and variability of the model were assessed using the coefficient of determination ($R^2$), which was calculated to be 0.95. This indicates that the model explains 95% of the total variation in the response, leaving only 5% unexplained. Thus, the model exhibits a high level of confidence in predicting the response.

The ANOVA results, including the p-value, sum of squares, mean square, model significance (F-value), and degrees of freedom (Table 4), reveal that the p-value for the regression model was below 0.05, indicating that the model terms are statistically significant at the 95% confidence level. This demonstrates the overall goodness of fit of the model. Additionally, the lack-of-fit p-value suggests that there is no significant lack of fit at the 0.05% level, further validating the model's statistical soundness. The adjusted coefficient of determination (adjusted $R^2$) was calculated to be 0.94, reflecting a strong agreement between the predicted model and the experimental data.

**Table 2. Central composite rotatable design arrangement and results.**

| Run | Independent variables | | | | | | Responses | |
|---|---|---|---|---|---|---|---|---|
| | Coded levels | | | Real values | | | Reduction yield | |
| | $X_1$ | $X_2$ | $X_3$ | Reduction temperature, in °C | $Ca/DyF_3$ molar ratio, in mol/mol | Reduction time, in h | Experimental* (Actual), in % | Calculated (Predicted), in % |
| 1 | -1 | -1 | -1 | 1400 | 1.95 | 0.50 | 71.4 | 71.6 |
| 2 | 1 | -1 | -1 | 1500 | 1.95 | 0.50 | 75.3 | 75.8 |
| 3 | -1 | 1 | -1 | 1400 | 2.25 | 0.50 | 78.1 | 78.1 |
| 4 | 1 | 1 | -1 | 1500 | 2.25 | 0.50 | 82.7 | 82.7 |
| 5 | -1 | -1 | 1 | 1400 | 1.95 | 1.00 | 74.8 | 74.8 |
| 6 | 1 | -1 | 1 | 1500 | 1.95 | 1.00 | 78.9 | 79.0 |
| 7 | -1 | 1 | 1 | 1400 | 2.25 | 1.00 | 80.2 | 79.7 |
| 8 | 1 | 1 | 1 | 1500 | 2.25 | 1.00 | 84.5 | 84.4 |
| 9 | -1 | 0 | 0 | 1400 | 2.10 | 0.75 | 78.4 | 78.7 |
| 10 | 1 | 0 | 0 | 1500 | 2.10 | 0.75 | 83.6 | 83.1 |
| 11 | 0 | -1 | 0 | 1450 | 1.95 | 0.75 | 80.3 | 79.4 |
| 12 | 0 | 1 | 0 | 1450 | 2.25 | 0.75 | 84.7 | 85.3 |
| 13 | 0 | 0 | -1 | 1450 | 2.10 | 0.50 | 83.2 | 82.5 |
| 14 | 0 | 0 | 1 | 1450 | 2.10 | 1.00 | 84.5 | 84.9 |
| 15 | 0 | 0 | 0 | 1450 | 2.10 | 0.75 | 83.8 | 84.3 |

*Experimental mean of five replications per batch.

**Table 3. Estimated regression coefficients for sequential model.**

| Source | Coefficient | Standard error | p-value |
|---|---|---|---|
| Model | 84.3378 | 0.418872 | 5.73439e-011 |
| $X_1$ | 2.21 | 0.246443 | 0.000287564 |
| $X_2$ | 2.95001 | 0.246443 | 7.17519e-005 |
| $X_3$ | 1.22 | 0.246443 | 0.00428328 |
| $X_1^2$ | -3.47222 | 0.485992 | 0.000834294 |
| $X_2^2$ | -1.97223 | 0.485992 | 0.00974683 |
| $X_3^2$ | -0.622238 | 0.485992 | 0.056602 |
| $X_1X_2$ | 0.112495 | 0.275532 | 0.099961 |
| $X_1X_3$ | -0.0124991 | 0.275532 | 0.065574 |
| $X_2X_3$ | -0.387508 | 0.275532 | 0.018609 |

Therefore, the results of the significance test, ANOVA, and evaluation metrics indicate that the quadratic model employed for the calciothermic reduction of $DyF_3$ is accurate and reliable. It effectively explains the variation in the response and demonstrates good agreement with the experimental data. The final predicted formula for the calciothermic reduction of $DyF_3$ to obtain metallic Dy, incorporating coded coefficients, is presented in Eq. (4):

$$Y=84.3+2.2X_1+3.0X_2+1.2X_3-3.5X_1^2-2.0X_2^2-0.6X_3^2+0.1X_1X_2-0.4X_2X_3 \quad (4)$$

**Table 4. The results of analysis of variance (ANOVA) of model.**

| Source | Degree of freedom | Sum of squares | Mean square | F-value | p-value | RSD |
|---|---|---|---|---|---|---|
| Regression | 9 | 233.784 | 25.976 | 42.7699 | 0.000 | 5.09666 |
| Residual | 5 | 3.03671 | 0.607341 | | | 0.779321 |
| Lack of fit | -- | -- | -- | -- | -- | -- |
| $R^2 = 0.95$; $R^2$ adj. = 0.94 | | | | | | |

In Fig. 4, a plot comparing the calculated reduction yield of $DyF_3$ by metallic calcium versus the experimental results is presented. The close distribution of the experimental data points around a straight line indicates a strong agreement between the predicted and actual results. This confirms that the RSM-CCF model for the calciothermic reduction is consistent with the experimental data.

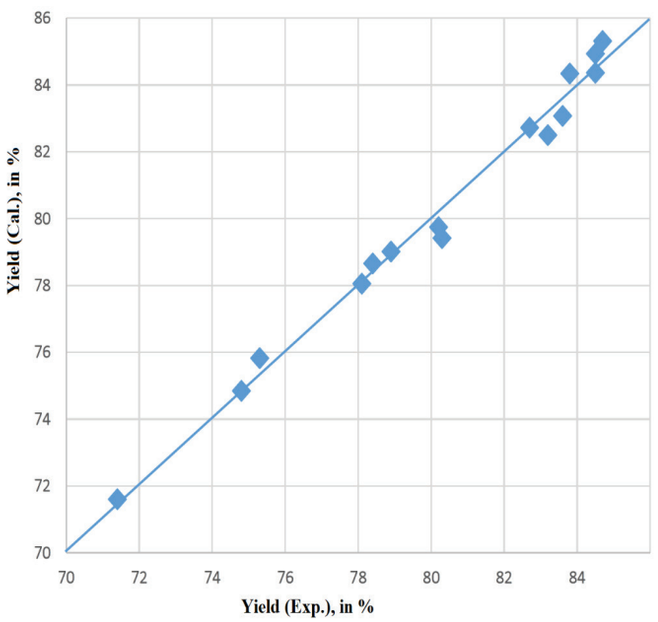


**Fig. 4. Linear correlation between calculated and experimental values for the calcinothermic reduction of $DyF_3$.**

### *3.3. Optimising the calcinothermic reduction of $DyF_3$*

#### *3.3.1. Interaction among factors*

From Eq. (4), several key insights can be drawn:

i. The contributions from the linear coefficients ($b_i$ of $X_i$) and quadratic coefficients ($b_i^2$ of $X_i^2$) on Y are far more significant than those from the interaction coefficients ($b_{ij}$ of $X_iX_j$). Therefore, the variables have largely independent effects on the response.

ii. The contributions from the coefficients $b_1$ and $b_1^2$ at the low level ($X_1$=-1) and high level ($X_1$=1) on Y were calculated as $b_0$-5.7 and $b_0$-1.3, respectively. This indicates a significant decrease in the reduction yield at $X_1$=-1. The highest reduction yield is achieved at temperatures between 1450 and 1460°C, with a calculated value of $b_0$=84.3 at $X_1$=0.

iii. The contributions from the coefficients $b_2$ and $b_2^2$ at the low level ($X_2$=-1) and high level ($X_2$=1) on Y were calculated as $b_0$-4.7 and $b_0$+0.8, respectively. This suggests a significant decrease in yield at $X_2$=-1, while the increase at $X_2$=1 is minimal. The highest yield is reached with Ca/$DyF_3$ molar ratios between 2.1 and 2.25.

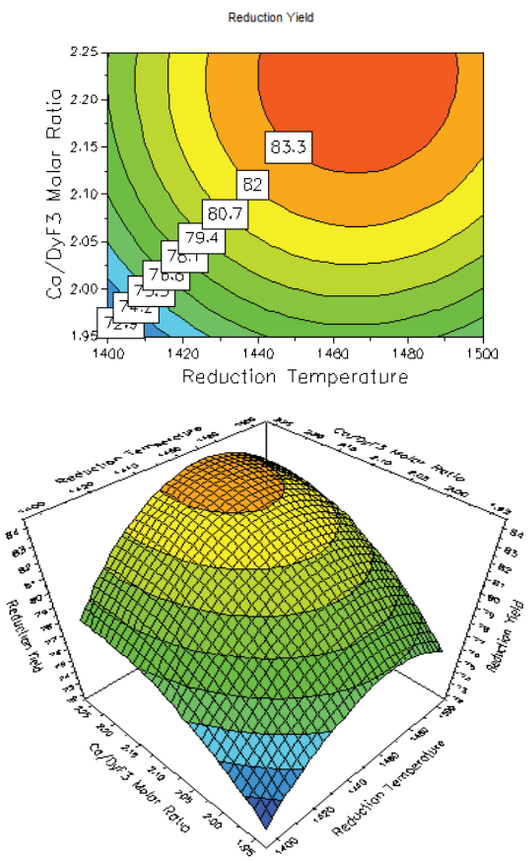


**Fig. 5. Contours and response surface of the reduction yield of $DyF_3$ by metallic calcium vs reduction temperature and Ca/$DyF_3$ molar ratio at a low level of the reduction time.**

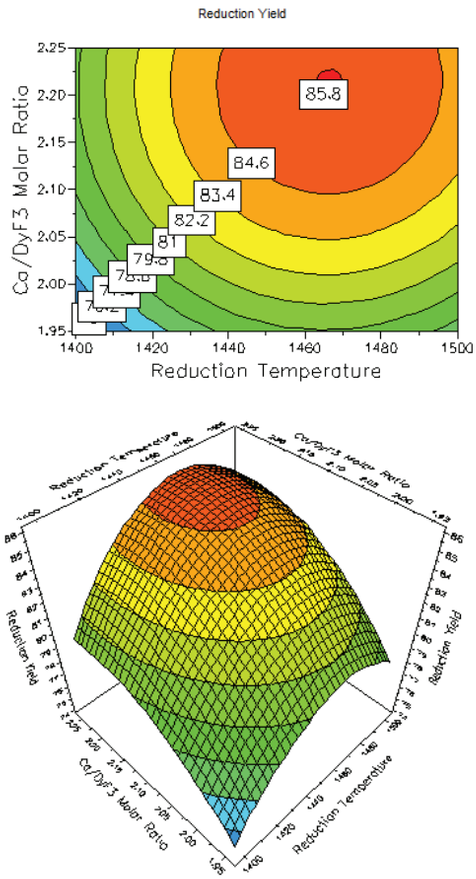


**Fig. 6. Contours and response surface of the reduction yield of $DyF_3$ by metallic calcium vs reduction temperature and Ca/$DyF_3$ molar ratio at centre level of the reduction time.**

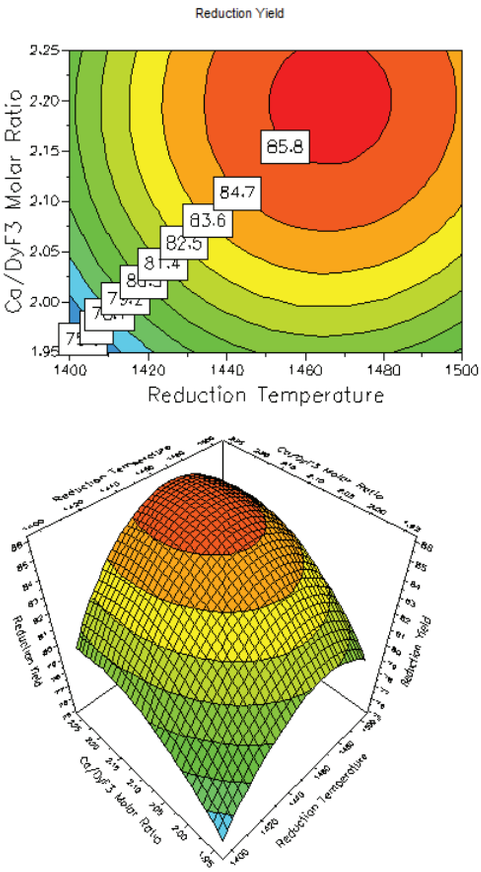


**Fig. 7. Contours and response surface of the reduction yield of $DyF_3$ by metallic calcium vs. reduction temperature and Ca/$DyF_3$ molar ratio at a high level of the reduction time.**

iv. The contributions from the coefficients $b_3$ and $b_3^2$ at the low level ($X_3$=-1) and high level ($X_3$=1) on Y were calculated as $b_0$-1.6 and $b_0$+0.4, respectively, indicating that reduction time has an insignificant effect on the yield.

The comprehensive analysis of these independent variables' contributions to the response shows that reduction temperature ($X_1$) has the most significant effect on the reduction yield (Y). Therefore, optimal conditions for the calciothermic reduction of $DyF_3$ are primarily determined by careful control of the reduction temperature. Although the Ca/$DyF_3$ molar ratio ($X_2$) and reduction time ($X_3$) also influence the process, their effects are comparatively weaker. To achieve the best overall performance, a balanced optimisation of all independent variables should be pursued, taking their relative importance and interdependence into account.

*3.3.2. Effect of factors on reduction yield*

The influence of experimental factors on the reduction yield of $DyF_3$ using metallic calcium is shown in Figs. 5-7. The reduction temperature positively affects the yield within the range of 1400 to 1450°C. However, at temperatures above 1450°C, the increase in yield is minimal, irrespective of the Ca/$DyF_3$ molar ratio or reduction time. A similar trend was observed for the effects of the Ca/$DyF_3$ molar ratio and reduction time on the yield, though the Ca/$DyF_3$ molar ratio had a stronger influence than reduction time.

Figure 8 provides a comprehensive visual overview of the effects of factors on the reduction yield. The linear positive effects of reduction temperature ($X_1$), time ($X_3$), and Ca/$DyF_3$ molar ratio ($X_2$) were quantified as 4.42±1.27, 2.44±1.27, and 5.90±1.27, respectively. Conversely, the quadratic negative effects of reduction temperature ($X_1^2$) and Ca/molar ratio ($X_2^2$) were -6.94±2.50 and -3.94±2.50, respectively. The remaining factors, including the quadratic influence of reduction time ($X_3^2$), the interactive influences of the reduction temperature and time ($X_1X_3$), the influence of the reduction temperature and the Ca/$DyF_3$ molar ratio ($X_1X_2$), and the influence of the Ca/$DyF_3$ molar ratio and reduction time ($X_2X_3$) on the $DyF_3$ calcinothermic reduction yield, were quantified as -0.02±1.42, 0.22±1.42, and -0.78±1.42, respectively. These influences exhibited larger uncertainties and were therefore deemed insignificant.

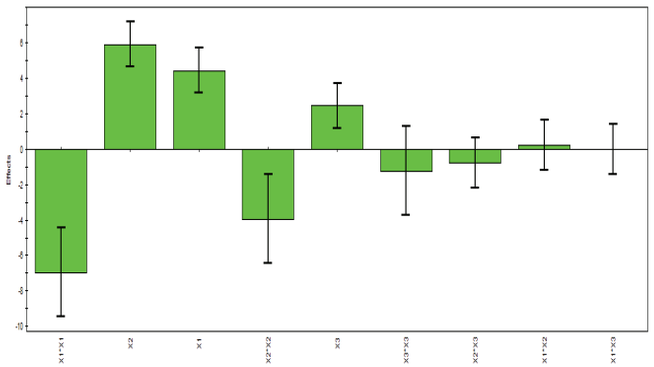

**Fig. 8. The effects of terms on the reduction yield of $DyF_3$ by metallic calcium.**

From these results, it can be concluded that reduction temperature exerts the strongest influence on the reduction yield, with values ranging from -6.94 to +4.42. The $Ca/DyF_3$ molar ratio has a weaker influence, ranging from -3.94 to +5.90, while reduction time has the weakest effect, at only +2.44. Combining the analysis of the contributions of the $b_{ij}$ coefficients with the analysis of the influences of the $X_i$ and $X_{ij}$ factors, it can be concluded that the calcinothermic reduction of to produce metallic Dy is predominantly controlled by reduction temperature.

*3.3.3. Optimising the calciothermic reduction of $DyF_3$*

To determine the most favourable conditions for achieving the highest yield in the calciothermic reduction of $DyF_3$, the RSM-CCF model was employed to explore desirable parameters within the design space. Using the RSM-CCF model in conjunction with MODDE 5.0 software, the optimal conditions for the calciothermic reduction process were identified. These optimal parameters consist of a reduction temperature of 1466°C, a reduction time of 0.9 hours, and a $Ca/DyF_3$ molar ratio of 2.2. Under these conditions, the maximum reduction yield of using metallic calcium achieved was 86.2% (Table 5).

**Table 5. Results of process optimisation and optimum levels of variables.**

| Reduction temperature (°C) | Ca/DyF3 molar ratio | Reduction time (hour) | Reduction yield | log(D) |
|---|---|---|---|---|
| 1466,39 | 2,2034 | 0,9399 | 86,1725 | -10 |
| 1466,25 | 2,2029 | 0,9381 | 86,1727 | -10 |
| 1466,26 | 2,2011 | 0,9397 | 86,1725 | -10 |
| 1480 | 2,25 | 1 | 85,662 | -1,2129 |
| 1460 | 2,16 | 0,75 | 85,5144 | -0,8992 |
| 1480 | 2,25 | 1 | 85,662 | -1,2129 |
| 1470 | 2,25 | 0,75 | 85,6892 | -1,2853 |
| 1450 | 2,16 | 1 | 85,6452 | -1,1708 |

However, optimising the calciothermic reduction process requires consideration of several key factors that can significantly influence the outcome. Striving for the highest yield alone is insufficient, as other critical aspects such as energy consumption, chemical usage, and waste management must also be accounted for. Thus, the predictive model should not focus solely on maximising yield, but rather consider trade-offs associated with these factors. To achieve optimal overall performance, the model should incorporate variables that are adaptable to cost, yield, profitability, and other significant parameters. This approach not only predicts outcomes but also guides the process towards the best possible results while minimising adverse environmental and resource impacts.

**Table 6. The calcinothermic reduction yield of $DyF_3$ calculated from Eq. (4).**

| No | $X_1$ (°C) | $X_2$ | $X_3$ (min) | Y (%) |
|---|---|---|---|---|
| 1 | 1450 | 2.15 | 40 | 84.7 |
| 2 | 1460 | 2.10 | 40 | 84.2 |
| 3 | 1460 | 2.15 | 40 | 85.0 |
| 4 | 1470 | 2.10 | 40 | 84.2 |
| 5 | 1470 | 2.15 | 40 | 85.0 |
| 6 | 1450 | 2.10 | 50 | 84.7 |
| **7** | **1450** | **2.15** | **50** | **85.4** |
| 8 | 1460 | 2.10 | 50 | 85.0 |
| **9** | **1460** | **2.15** | **50** | **85.7** |
| 10 | 1470 | 2.10 | 50 | 85.0 |
| 11 | 1470 | 2.15 | 50 | 85.7 |

Table 6 presents the calciothermic reduction yield of $DyF_3$, calculated using Eq. (4). To optimise the performance of the calciothermic reduction process, factors such as energy consumption, chemical usage, waste treatment, and the reduction yield must be carefully considered. Based on the results, it is recommended to set the reduction temperature between 1450 and 1460°C, with a reduction time of 50 minutes, and maintain a $Ca/DyF_3$ molar ratio of 2.15. This optimisation strategy, derived from the experimental data of samples 7 and 9 in Table 6, is expected to result in an efficient reduction process with minimal energy and chemical consumption, effective waste treatment, and a high reduction yield.

By carefully considering these factors, an optimised calciothermic reduction process can be developed that meets both industrial and environmental standards. Following the identification of the optimised conditions for the calciothermic reduction of $DyF_3$, additional experiments were conducted to validate the model's accuracy in producing metallic Dy. The optimised parameters were applied in further experiments, and the resulting reduction yield was compared to the model's predicted yield. The outcomes were highly satisfactory, confirming the model's ability to accurately predict the reduction yield of $DyF_3$ for metallic Dy production. This successful validation represents a significant step towards the practical implementation of

the calciothermic reduction process on a larger scale, facilitating the preparation of metallic Dy with high yields while minimising energy and chemical usage.

## 4. Conclusions

The calciothermic reduction of $DyF_3$ to produce metallic Dy was examined using a response surface methodology (RSM) based on a central composite face (CCF) design. The developed RSM-CCF model demonstrated a strong correlation with the experimental results, underscoring its effectiveness for metallic Dy preparation. Analysis revealed that the reduction temperature had the most significant impact on the reduction yield, highlighting its critical role in the optimisation process.

Considering factors such as energy consumption, chemical usage, waste management, and reduction yield, the parameters for the calciothermic reduction were optimised. The optimal conditions identified were a reduction temperature range of 1450 to 1460°C, a reduction time of 50 minutes, and a Ca/$DyF_3$ molar ratio of 2.15. Under these conditions, a maximum reduction yield of 85.7% was achieved.

The successful outcomes of the testing further validate the proposed model's effectiveness. This model offers promising potential for advancing the development of comprehensive processing technologies for the production of metallic Nd, Dy, Tb, and Y from Yen Phu xenotime concentrate.

## CRediT author statement

Nguyen Trong Hung: Methodology, Conceptualisation, Idea, Writing - Reviewing and Editing; Nguyen Thanh Thuy: Investigation, Visualisation; Le Ba Thuan: Supervision, Methodology.

## ACKNOWLEDGEMENTS

This research was financially supported by the Vietnam Ministry of Science and Technology under the projects 2022-2023 (code DTCB.11/19/VCNXH).

## COMPETING INTERESTS

The authors declare that there is no conflict of interest regarding the publication of this article.

## REFERENCES

[1] C.K. Gupta, N. Krishnamurthy (2005), *Extractive Metallurgy of Rare Earths*, CRC Press, 484pp.

[2] P. Zapp, J. Marx, A. Schreiber, et al. (2018), "Comparison of dysprosium production from different resources by life cycle assessment", *Resources, Conservation & Recycling*, **130**, pp.248-259, DOI: 10.1016/j.resconrec.2017.12.006.

[3] S. Hoenderdaal, L.T. Espinoza, F.M. Weidemann, et al. (2013), "Can a dysprosium shortage threaten green energy technologies?", *Energy*, **49**, pp.344-355, DOI: 10.1016/j.energy.2012.10.043.

[4] V.A. Ivanov, A.S. Dedyukhin, I.B. Polovov, et al. (2015), "Fabrication of rare-earth metals by metallothermic reduction: Thermodynamic modeling and practical realization", *AIP Conference Proceedings 2015*, DOI: 10.1063/1.5055106.

[5] C.K. Gupta, N. Krishnamurthy (2013), "Oxide reduction processes in the preparation of rare-earth metals", *Minerals & Metallurgical Processing*, **30**, pp.38-44, DOI: 10.1007/BF03402339.

[6] J.L. Moriarty (1968), "The industrial preparation of the rare earth metals by metallothermic reduction", *The Journal of The Minerals, Metals & Materials Society*, **20**, pp.41-45, DOI: 10.1007/BF03378760.

[7] B.J. Beaudry, K.A. Gschneidner (1978), "Chapter 2: Preparation and basic properties of the rare earth metals", *Handbook on the Physics and Chemistry of Rare Earths*, **1**, pp.173-232, DOI: 10.1016/S0168-1273(78)01006-5.

[8] H. Liu, Y. Zhang, Y. Luan (2020), "Research progress in preparation and purification of rare earth metals", *Metals*, **10(10)**, DOI: 10.3390/met10101376.

[9] A. Mukherjee, A. Awasthi, N. Krishnamurthy (2016), "Studies on calcium reduction of yttrium fluoride", *Mineral Processing and Extractive Metallurgy*, **125(1)**, pp.26-31, DOI: 10.1179/1743285515Y.0000000017.

[10] F.E. Block (1964), *Preparation of Yttrium and Rare Earth Metals by Metallothermic Reduction*, Thesis of Oregon State University, 118pp.

[11] T.M. Riedemann (2011), *High Purity Rare Earth Metals Preparation*, MPC Rare Earth Materials Section, https://slideplayer.com/slide/2859004/, accessed 7 January 2023.

[12] T.H. Nguyen, B.T. Le, T.T. Nguyen (2021), "Study on the fluorination of dysprosium oxide by ammonium bifluoride for the preparation of dysprosium fluoride", *Vietnam Journal of Science and Technology - MOST*, **63(8)**, pp.9-13, DOI: 10.31276/VJST.63(8).09-13 (in Vietnamese).

[13] N.T. Hung, N.T. Thuy, L.B. Thuan, et al. (2021), "Anhydrous oxygen-free rare earth material preparation and characterization", *Materials Today Chemistry*, **22**, DOI: 10.1016/j.mtchem.2021.100608.

[14] T.H. Nguyen, T.T. Nguyen, B.T. Le, et al. (2022), "The wet preparation and dehydration of terbium fluoride salt for terbium metal processing", *Vietnam Journal of Science and Technology - MOST*, **64(8)**, pp.47-52, DOI: 10.31276/VJST.64(8).47-52 (in Vietnamese).

[15] N.T. Hung, L.B. Thuan, T.C. Thanh, et al. (2020a), "Optimization of sulfuric acid leaching of a Vietnamese rare earth concentrate", *Hydrometallurgy*, **191**, DOI: 10.1016/j.hydromet.2019.105195.

[16] N.T. Hung, L.B. Thuan, T.C. Thanh, et al. (2020b), "Separation of thorium and uranium from xenotime leach solutions by solvent extraction using primary and tertiary amines", *Hydrometallurgy*, **198**, DOI: 10.1016/j.hydromet.2020.105506.

[17] N. Aoyagi, T.T. Nguyen, Y. Kumagai, et al. (2020), "Spectroscopic studies of mössbauer, infrared, and laser-induced luminescence for classifying rare-earth minerals enriched in iron rich deposits", *ACS Omega*, **5(13)**, pp.7096-7105, DOI: 10.1021/acsomega.9b03247.

[18] N.T. Hung, L.B. Thuan, T.C. Thanh, et al. (2022), "Selective recovery of thorium and uranium from leach solutions of rare earth concentrates in continuous solvent extraction mode with primary amine N1923", *Hydrometallurgy*, **213**, DOI: 10.1016/j.hydromet.2022.105933.